Acta Cryst C STRUCTURAL CHEMISTRY

ISSN 2053-2296

Structure and charge analysis of a cyclic aluminium hydride: *cyclo*-1,5-bis-μ-dimethylamino-3,7-di-μ-hydrido-2,4,6,8-tetrakis(dimethylaluminium)

Peter W. R. Corfield* and Joshua Schrier

Department of Chemistry, Fordham University, 441 East Fordham Road, Bronx, New York 10458, USA. *Correspondence e-mail: pcorfield@fordham.edu

Received 28 August 2022
Accepted 25 November 2022

Edited by A. Sarjeant, Bristol-Myers Squibb, USA

Keywords: crystal structure; hydride bridge; organoaluminium; DFT; charge determination.

CCDC reference: 2222230

Supporting information: this article has supporting information at journals.iucr.org/c

The title compound, $[Al_4(CH_3)_8(C_2H_7N)_2H_2]$, crystallizes as eight-membered rings with $-(CH_3)_2Al-(CH_3)_2N-(CH_3)_2Al-$ moieties connected by single hydride bridges. In the X-ray structure, the ring has a chair conformation, with the hydride H atoms being close to the plane through the four Al atoms. An optimized structure was also calculated by all-electron density functional theory (DFT) methods, which agrees with the X-ray structure but gives a somewhat different geometry for the hydride bridge. Charges on the individual atoms were determined by valence shell occupancy refinements using *MoPro* and also by DFT calculations analyzed by several different methods. All methods agree in assigning a positive charge to the Al atoms, negative charges to the C, N, and hydride H atoms, and small positive charges to the methyl H atoms.

1. Introduction

In E. P. Schram's early studies on the organometallic chemistry of aluminium, his group analyzed the products of the reaction between dimethylaminoboranes and methyl aluminium hydrides (Hall & Schram, 1969; Schram & Hall, 1971; Schram *et al.*, 1969). In further work, the reaction of dimethylaminoborane, $[(CH_3)_2NBH_2]_2$, with trimethylaluminium led to the isolation of a solid crystalline material. Analysis of single-crystal X-ray data collected in 1970–71 characterized the molecule that had been formed as *cyclo*-1,5-bis-μ-dimethylamino-3,7-di-μ-hydrido-2,4,6,8-tetrakis(dimethylaluminium), $Al_4(CH_3)_8[N(CH_3)_2]_2H_2$, **1** (Scheme 1). The molecule consists of an eight-membered ring containing singly-bridged hydride atoms, one of the first examples of such bridging at that time. Circumstances prevented completion of the refinement, although the molecular structure without atomic parameters was described in a paper on the chemical reaction (Glore *et al.*, 1972). We now present details of this X-ray study based upon refinement of the 1971 data, together with an atomic charge–density analysis, and we compare the structure and charges with those found from a theoretical study.

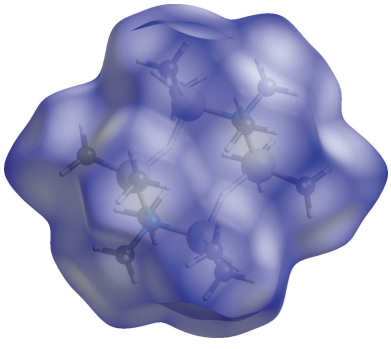

2. Experimental

2.1. Synthesis and crystallization

Details of the vacuum line synthesis of the title compound, its purification by vacuum sublimation, and its chemical and spectroscopic analyses are given in Glore *et al.* (1972). The data crystal was mounted in a 0.5 mm thin-walled capillary tube in a dry-box and sealed under a nitrogen atmosphere.

2.2. Refinement details

Crystal data, data collection and structure refinement details are summarized in Table 1. Since the original data reduction listed structure factors, F, rather than the F^2 values used in today's refinements, the 29 cases where the averaged values of the net intensity were less than zero had been recorded with F values of zero. On preparing *hkl* files with F^2 values, these 29 zero values were replaced with $F^2 = \sigma(F^2) = 0.63S$, where S was the average value of $\sigma(F^2)$ for reflections with $F^2 < 3\sigma(F^2)$ in the same θ range. $0.63S$ was chosen as the most probable value of the missing reflection.

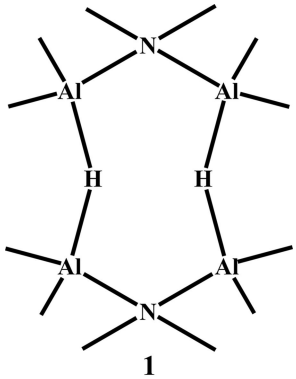

1
Scheme 1

In refinements with *SHELXL2018*, the methyl H atoms were constrained to tetrahedral geometry, with bond lengths of 0.96 Å and displacement parameters set to 1.5 times the average U value of the methyl C atom. A torsion angle was also refined for each methyl group. The bridging H atom was allowed to refine freely with an isothermal displacement parameter. Standard scattering factors were used and an extinction parameter was refined.

In the *MoPro* charge refinements, scattering factors are computed from Slater-type wave functions tabulated by Thakkar (Koga *et al.*, 1999). The methyl H atoms were constrained to tetrahedral geometry, with bond lengths of 1.099 Å and displacement parameters set to 1.5 times the average U value of the methyl C atom, but no torsion angles were refined. The hydride H atom was refined anisotropically in order to distinguish it from other H atoms and to refine its occupancy factor; the mean-square atomic displacements found were: 0.07, 0.10, and 0.15. No positional parameter differences of more than 2σ were seen between the *SHELX* and *MoPro* refinements.

Table 1
Experimental details.

Crystal data	
Chemical formula	$[Al_4(CH_3)_8(C_2H_7N)_2H_2]$
M_r	318.36
Crystal system, space group	Monoclinic, $P2_1/n$
Temperature (K)	295
a, b, c (Å)	14.175 (13), 10.378 (11), 7.692 (7)
β (°)	90.74 (4)
V (Å^3)	1131.5 (19)
Z	2
Radiation type	Cu $K\alpha$
μ (mm^{-1})	1.83
Crystal size (mm)	0.48 × 0.40 × 0.17
Data collection	
Diffractometer	Picker 4-circle diffractometer
Absorption correction	Gaussian (Busing & Levy, 1957); 8 × 8 × 8 grid
T_{min}, T_{max}	0.46, 0.71
No. of measured, independent and observed [$I > 2\sigma(I)$] reflections	3367, 1582, 1352
R_{int}	0.068
θ_{max} (°)	58.0
$(\sin\theta/\lambda)_{max}$ (Å^{-1})	0.550
Refinement	
$R[F^2 > 2\sigma(F^2)]$, $wR(F^2)$, S	0.039, 0.110, 1.07
No. of reflections	1582
No. of parameters	93
H-atom treatment	H atoms treated by a mixture of independent and constrained refinement
$\Delta\rho_{max}$, $\Delta\rho_{min}$ (e Å^{-3})	0.18, −0.20

Computer programs: Corfield & Gainsford (1972), Corfield *et al.* (1973), *SHELXL2018* (Sheldrick, 2015), *ORTEPIII* (Burnett & Johnson, 1996), *ORTEP-3* (Farrugia, 2012), and *publCIF* (Westrip, 2010).

3. Results and discussion

3.1. Description of the X-ray structure

Fig. 1 shows atomic displacement ellipsoids for the asymmetric unit and the atom numbering. The title compound crystallizes as eight-membered rings with hydride H atoms joining two Me_2Al–Me_2N–Me_2Al moieties. Overall, the molecule has a chair conformation. The Al and hydride H atoms are essentially coplanar, with the H atoms just 0.06 (2) Å from the central plane of the four Al atoms, and the N atoms displaced 0.841 (2) Å above and below this Al_4 plane. The dihedral angle between the Al_4 central plane and the Al—N—Al edge plane is 54.3 (1)°, a little larger than the comparable angle of 49.2° in cyclohexane. Methyl groups C1, C3 and C5 are equatorial, and methyl groups C2, C4, and C6 are axial. The Al—N distances are normal, at 1.941 (3) and 1.941 (4) Å, while the Al—H distances are 1.657 (19) and 1.692 (19) Å. The internal angles at the Al atoms are 95.8 (7) and 96.8 (7)°, while at the N atom, the internal angle is 115.49 (10)°. The Al—H—Al angle deviates significantly from

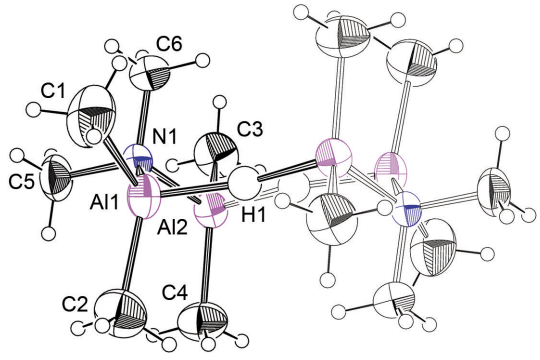

Figure 1
Displacement ellipsoid plot of the title compound, with ellipsoids at the 50% probability level, except that the methyl H atoms are plotted at an arbitrary scale. The asymmetric unit is highlighted in bold.

Table 2
Intermolecular interaction energies in kJ mol^{-1} calculated with *CrystalExplorer* using electron density calculated with B3LYP/6-31G(d,p).

Electronic (E_{ele}), polarization (E_{pol}), dispersion (E_{dis}), and repulsion energies (E_{rep}) are scaled with factors 1.057, 0.740, 0.871, and 0.618, respectively, when combined to form the total energy of interaction. R is the distance between molecular centroids, in Å.

	N	Sym	R	E_{ele}	E_{pol}	E_{dis}	E_{rep}	E_{total}
1	2	*c trans*	7.69	−4	−2	−28	8	−26
2	4	*n*-glide	9.55	0	−1	0	0	−1
3	4	*n*-glide	9.63	−2	−1	−21	7	−18
4	2	*b trans*	10.38	−4	−1	−14	2	−16

linearity, at 153 (1)°, with the H atoms moved towards the center of the ring, reducing the H···H distance to 2.52 (4) Å, close to the sum of the van der Waals radii for the H atoms.

3.2. Supramolecular features and Hirshfeld surface analysis

The molecules pack in a centered arrangement with regard to the unit cell, as shown in Fig. 2. All the shortest intermolecular contacts are due to H···H contacts between methyl groups, with H···H contact distances greater than twice the van der Waals radius for hydrogen. The molecule was analyzed by the Hirshfeld procedure (Spackman *et al.*, 2009; Tan *et al.*, 2019) using *CrystalExplorer* (Turner *et al.*, 2017). The d_{norm} plots in Figs. 3(*a*) and 3(*a*) are all blue, again indicating no contacts less than the sum of the van der Waals radii. The surface tends to be flattened at the methyl groups. The fingerprint plot is featureless, in line with the lack of strong intermolecular interactions, and all contacts at the surface are H···H contacts. Intermolecular interaction energies calculated with *CrystalExplorer* are given in Table 2. As can be seen, the dominant interactions are due to dispersion forces between the H atoms, with only minor contributions from Coulombic, polarization, and exchange–repulsion forces.

3.3. Database survey

There are over 7000 crystal structures with a metal hydride bridge in the Cambridge Structural Database (CSD; Groom *et al.*, 2016). Of these, 52 hits were found that contain a singly-hydride-bridged pair of Al atoms and for which atomic coordinates were available. Six of these cases contained μ_3- or μ_4-bridging hydrides, while the remaining 46 hits, with 64 hydride geometries, contain a single μ_2-bridging hydride atom. The Al—H distances range from 1.46 to 1.90 Å, with a mean of 1.73 Å. The Al—H distances in the present structure of 1.657 (19) and 1.692 (19) Å fall at the center of this range. The

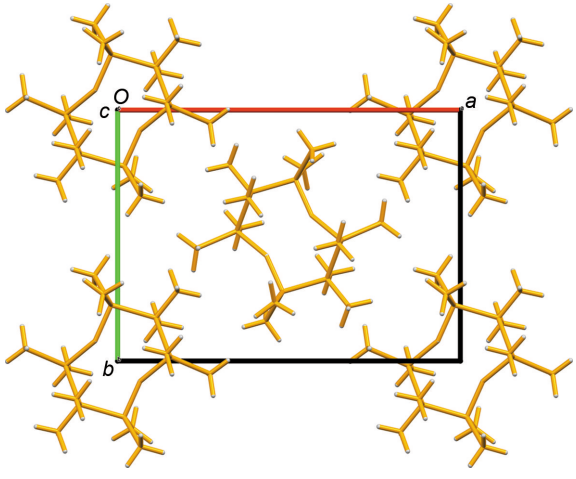

Figure 2
Packing diagram showing the projection down the *c* axis.

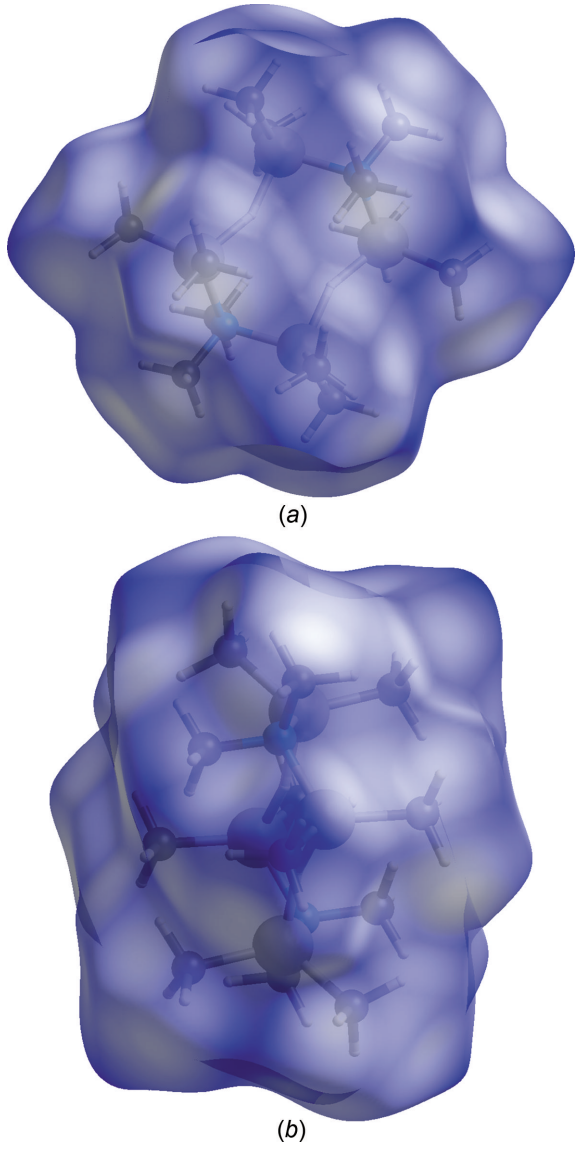

Figure 3
Hirshfeld d_{norm} surface (*a*) near the normal to the Al plane and (*b*) perpendicular to the view in part (*a*).

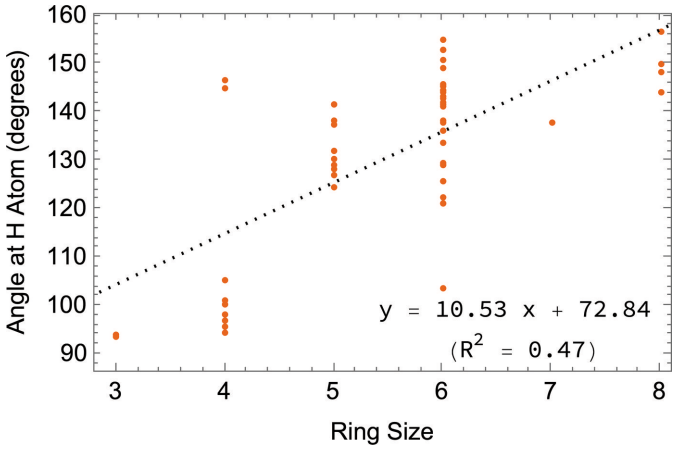

Figure 4
Chart showing the variation of hydride bond angles with ring size.

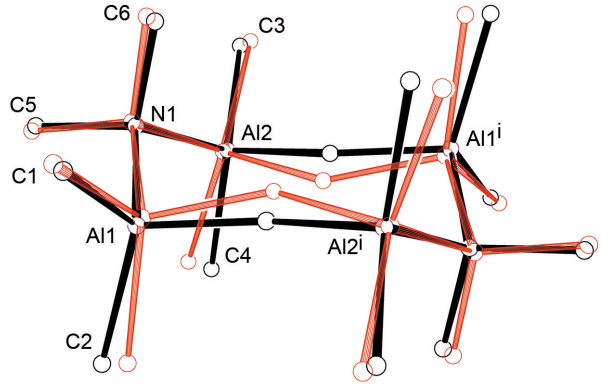

Figure 5
The X-ray (black) and DFT (red) structures displayed on common Al_4-based axes. Methyl H atoms are not included. [Symmetry code: (i) $-x+1$, $-y+1$, $-z+1$.]

angles at the hydride anion vary widely, from 94 to 180°. The hydride bond angle is clearly more flexible than the typical bond angle between normal two-center covalent bonds. One factor affecting this angle must be that the hydride bridge is often part of a ring of atoms that contain the Al—H—Al moiety, with ring sizes varying widely. The chart in Fig. 4 based on 56 cyclic structures shows a rough correlation between the hydride angle and the ring size, with the smallest angles generally occurring when the Al—H—Al bridge is in a three- or four-membered ring, and the larger angles being associated with larger ring sizes. (Seven of the other structures were acyclic and one had a very large ring which was not plotted.) A further factor in the wide range of bond angles observed is the presence of many Al cluster compounds, for which the bonding pattern is complicated. Hydride bond angles for eight-membered rings, for which there should be few stereochemical constraints, as in the present structure, range from 144 to 157°. The Al—H—Al bond angle in the present structure of 153 (1)° falls nicely in this range.

3.4. Theoretical structure calculations

Density functional theory (DFT) calculations were performed on the neutral gas-phase $C_{12}H_{38}Al_4N_2$ building unit, at the unrestricted B97-2/aug-cc-pvDZ level using *GAUSSIAN16* (Frisch *et al.*, 2019). The optimized structure and charges are archived at the NOMAD repository (doi: 10.17172/NOMAD/2022.08.27-1). Previous work found that this level of theory gave the best description of the geometry and thermochemistry of Al_nN_m and Al_nH_m clusters (Loukhovitski *et al.*, 2016, 2018). The gas-phase structure of the DFT calculations was expected to match the X-ray structure, since the crystal intermolecular forces are weak. As a check, DFT calculations were also made for dimers along the z axis and the n-glide plane directions, with insignificant changes in geometry and charge.

We compare the X-ray structure and the fully optimized DFT structure in Fig. 5, where methyl H atoms have been excluded. The overall match is good, with bond angles between non-H atoms all agreeing within 1–2°, and bond lengths differing by no more than 0.03 Å, except for the Al—N bond length, which is 2.00 Å in the DFT structure *versus* 1.94 Å in the X-ray structure. Other differences include: (*a*) X-ray C—H distances show the expected shortening compared with those in the DFT structure (0.96 *versus* 1.10 Å), due to scattering of X-rays from the electron density, which for bonded H atoms is pulled into the bond and away from the nucleus; (*b*) torsion angles for the methyl groups are closer to the staggered conformation in the optimized structure, whereas the C2 and C3 methyl groups on the Al atoms are twisted 15 and 23° from the staggered conformation, presumably due to interactions in the crystal; (*c*) the DFT and X-ray hydride H-atom positions are 0.41 Å apart. The DFT Al—H—Al angle is 145°, smaller than the angle of 153 (1)° in the X-ray structure, while the hydride H atom is 0.27 Å above the Al_4 plane in the DFT structure, compared with 0.06 (2) Å in the X-ray structure. The differences are illustrated in Fig. 6, which also shows an F_o–F_c Fourier synthesis where the hydride contribution to F_c has been subtracted out. We can understand the hydride bridge in simple terms as a bent $3c$—$2e$ bond where both electrons come from the H^- ion, as reviewed recently by Parkin (2019). Presumably, much of the difference between the hydride geometry from the DFT calculations and from the X-ray crystal structures is again an artifact due to the electron density from the bridging H atom being pulled into the two bonds.

3.5. Charge density analysis: X-ray and theoretical

3.5.1. X-ray charge analysis. The structure was refined by the conventional independent atom model (IAM) using *SHELXL2018* (Sheldrick, 2015). These are the parameters given in the CIF file associated with this article. The resulting IAM model was then refined along with valence shell population parameters by *MoPro* (Jelsch *et al.*, 2005). Scattering factors used were of the form $f = f_{core} + p\kappa^3 f_{val}$, where p is a refined parameter, constrained to be the same for chemically equivalent atoms and by a neutrality requirement, and κ is the radial expansion/contraction parameter, set at 1.16 for all

Table 3
Partial charges for the chemically independent atoms in $Al_4(CH_3)_6N_2H_2$.

The *K* values for the two *MoPro* results are given in the text.

Method	*MoPro*		Theoretical			
Atom	Fixed *K*	Varied *K*	Hirshfeld	cm^5	ESP	NBO
Al	1.01 (9)	1.48 (10)	0.45	0.29	0.91	1.72
N	−0.42 (4)	−0.36 (4)	−0.14	−0.42	−0.05	−1.09
H(bridging)	−0.45 (5)	−0.59 (5)	−0.13	0.00	−0.34	−0.52
C(Al methyl)	−0.95 (4)	−1.01 (5)	−0.27	−0.44	−0.81	−1.22
C(N methyl)	−0.48 (5)	−0.50 (5)	−0.04	−0.19	−0.41	−0.34
H(Al methyl)	0.27 (2)	0.24 (2)	0.02	0.10	0.15	0.21
H(N methyl)	0.07 (2)	0.02 (3)	0.05	0.13	0.14	0.19

methyl H atoms and at 1.00 for the other atoms, as suggested by *MoPro*. Refinement of the positional and displacement parameters and of the *p* values was carried out in ten alternating cycles. *MoPro R* values fell from R_1(all) = 0.0544 to 0.0489, and R_w from 0.1270 to 0.1082. For just nine extra variables, this is a statistically significant drop, according to Hamilton's *R*-factor significance test (Hamilton, 1965). The *R* values for *MoPro* were somewhat different from those in *SHELXL*, mainly due to the use of different scattering factors and a slightly different model. Partial charges derived from the *p* values are shown in Table 3. A CIF file from the *MoPro* refinements is given in the supporting information.

We had fixed κ values at 1.16 for H and 1.00 for the other atoms, as we would not expect κ values to be well defined by refinements with our limited data set. The refined *p* values, however, are expected to be correlated with the κ values. We have therefore explored the effects of variations in κ for the methyl H atoms, κ(H), first by carrying out refinements to convergence with fixed κ(H) values ranging from 1.06 to 1.26, and then by refining κ values. Refinements indicated that

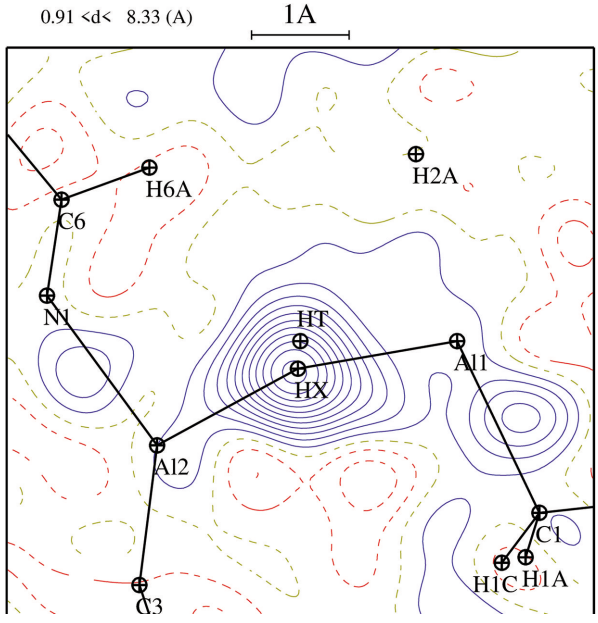

Figure 6
X-ray electron density in the Al—H—Al plane. The F_c values were from the refined structure less the hydride-atom contribution. HX gives the position of the hydride atom from the X-ray analysis and HT gives the DFT position. The contours are at 0.05 e $Å^{-3}$.

κ(Al), κ(N) or κ(H^-) did not differ significantly from unity, and so these values were fixed at unity. A sample refinement where only κ(H) and κ(C) were allowed to vary converged with κ(H) = 1.05 (1) and κ(C) = 0.98 (1), with slightly higher *R* values. Partial charges corresponding to the *p* values from this refinement are also given in Table 3. Variations between those obtained from the fixed and from the refined κ values can give an idea of the uncertainties in our partial charges.

In all refinements, the C—H bond lengths were reset to the neutron diffraction value of 1.099 Å for Csp^3 (Allen & Bruno, 2010), as is usual for such studies (Stewart, 1970; Meenashi *et al.*, 2020). Significant differences in occupancies were observed if C—H distances were left at the X-ray values of 0.96 Å, as used in the X-ray analysis. However, when a C—H distance of 1.078 Å was used, the values used in *CrystalExplorer*, no change was more than 1σ. The X-ray charges are not sensitive to small changes in the neutron C—H bond lengths.

3.5.2. Theoretical charge analysis. Although the total electron density is a well-defined quantity in quantum mechanics and density functional theory, there is no unique decomposition of the electron density into atom-centered domains, and there are many different atomic charge assignment methods, which can give quantitatively and even qualitatively different results (Contreras *et al.*, 2017). Therefore, one expects only qualitative agreement amongst the different calculation methods and with the experimental results. Results in Table 3 show atomic partial charge decompositions using Hirshfeld, CM5, Merz–Kollman electrostatic potential, and natural bond orbital (NBO) methods using the optimized structure. Only small (±0.01 e) differences in the results were found when calculations were conducted with atoms fixed to the crystallographic coordinates, or in the presence of dimers along the *z* axis and glide-axis directions.

The variations between these predictions can be explained as follows:

(i) The Hirshfeld method (also known as a stakeholder or shareholder method) assigns the total electron density to atoms proportional to the relative neutral pro-atomic density; Hirshfeld charges are conceptually most similar to those from crystallographic analysis, but tend to underestimate the magnitude of the charge.

(ii) Charge Model 5 (CM5) adds an empirical correction to the Hirshfeld charges to reproduce experimental dipole moments. Although the CM5 training set included Al-containing compounds, the parameterization did not consider

Al—N or Al—H—Al bonds, and so the empirical correction parameters may not be applicable for all of the types of atoms in our structure. Indeed, we see the largest discrepancies with the charge on the hydride.

(iii) Electrostatic potential (ESP) methods assign point charges to the atoms that best reproduce the molecular electrostatic potential; we used the Merz–Kollman (MK) algorithm, although other variations exist (Francl & Chirlian, 2000). A general problem with ESP methods is that atoms buried within the interior of a molecule may be assigned non-physical partial charges as they have minimal contribution to the electrostatic potential surface. This could be an issue in our present application, as both the van der Waals spheres of the hydride H atoms and the Al atoms (surrounded by methyl groups) are obscured.

(iv) Natural Bond Orbital (NBO) methods express the wavefunction in terms of maximally localized atomic orbital-like basis functions whose core orbitals are close to doubly occupied and whose valence orbitals have single occupancy. This is conceptually most similar to the way formal charges are assigned when analyzing Lewis structures (McArdle, 2019). As such, they may overemphasize charge transfer.

3.5.3. Results. Despite the variations between the various theoretical methods, the data shown in Table 3 indicate qualitative agreement of the partial charges obtained from the *MoPro* refinements and by the DFT calculations. Both the experimental and all theoretical assignments suggest substantial positive charges on the Al atoms, negative charges of about half an electron on the N and bridging H atoms, and negative charges on the C(Al) atoms that are much more negative than on the C(N) atoms. There are small positive charges on the methyl H atoms. These results are consistent with the Al—N and Al—C electronegativity differences of 1.0 and 1.5, which would indicate a polar Al—N and a more polar Al—C bond. The negative charge found for the bridging H atom is consistent with its characterization as a hydride. The *MoPro* refinement distinguishes between charges on the methyl H atoms on the Al and N atoms, whereas the charges estimated from the DFT calculations do not distinguish between these H atoms, although the total charges assigned to the Al-bound and N-bound methyl groups are different in each of the DFT calculations. A distinction between the Al-bound and the N-bound methyl groups might be expected on chemical grounds. The limited Cu $K\alpha$ resolution of the data used in this study forces the *MoPro* results to be limited to the spherical independent atom model, and the charges are not as well defined as we would wish; use of data collected with a shorter wavelength would have allowed a more sophisticated model by the *MoPro* program.

Acknowledgements

We are grateful to J. D. Glore, who mounted the crystal and assisted in the X-ray data collection at the Ohio State University. We thank Michael Zdilla of Temple University for valuable suggestions, and also a reviewer, who advised the use of the κ values in the *MoPro* refinements. We acknowledge use of the computational resources of the Mercury consortium (https://mercuryconsortium.org/) under NSF grant No. CNS2018427.

Funding information

Funding for this research was provided by: National Science Foundation Equipment Grant (award No. GP8534); National Science Foundation (grant No. DMR-1928882); Henry-Dreyfus Teacher-Scholar (award No. TH-14-010).

References

Allen, F. H. & Bruno, I. J. (2010). *Acta Cryst.* B**66**, 380–386.
Burnett, M. N. & Johnson, C. K. (1996). *ORTEPIII*. Report ORNL6895. Oak Ridge National Laboratory, Tennessee, USA.
Busing, W. R. & Levy, H. A. (1957). *Acta Cryst.* **10**, 180–182.
Contreras, R., Domingo, L. R. & Silvi, B. (2017). *Electron Densities: Population Analysis and Beyond*, in *Encyclopedia of Physical Organic Chemistry*, edited by Z. Wang. Hoboken, New Jersey: John Wiley & Sons Inc.
Corfield, P. W. R., Dabrowiak, J. C. & Gore, E. S. (1973). *Inorg. Chem.* **12**, 1734–1740.
Corfield, P. W. R. & Gainsford, G. J. (1972). Local versions of standard programs, written at the Ohio State University.
Farrugia, L. J. (2012). *J. Appl. Cryst.* **45**, 849–854.
Francl, M. M. & Chirlian, L. E. (2000). *Rev. Comput. Chem.* **14**, 1–31.
Frisch, M. J., Trucks, G. W., Schlegel, H. B., Scuseria, G. E., Robb, M. A., Cheeseman, J. R., Scalmani, G., Barone, V., Petersson, G. A., Nakatsuji, H., Li, X., Caricato, M., Marenich, A. V., Bloino, J., Janesko, B. G., Gomperts, R., Mennucci, B., Hratchian, H. P., Ortiz, J. V., Izmaylov, A. F., Sonnenberg, J. L., Williams-Young, D., Ding, F., Lipparini, F., Egidi, F., Goings, J., Peng, B., Petrone, A., Henderson, T., Ranasinghe, D., Zakrzewski, V. G., Gao, J., Rega, N., Zheng, G., Liang, W., Hada, M., Ehara, M., Toyota, K., Fukuda, R., Hasegawa, J., Ishida, M., Nakajima, T., Honda, Y., Kitao, O., Nakai, H., Vreven, T., Throssell, K., Montgomery, J. A. Jr, Peralta, J. E., Ogliaro, F., Bearpark, M. J., Heyd, J. J., Brothers, E. N., Kudin, K. N., Staroverov, V. N., Keith, T. A., Kobayashi, R., Normand, J., Raghavachari, K., Rendell, A. P., Burant, J. C., Iyengar, S. S., Tomasi, J., Cossi, M., Millam, J. M., Klene, M., Adamo, C., Cammi, R., Ochterski, J. W., Martin, R. L., Morokuma, K., Farkas, O., Foresman, J. B. & Fox, D. J. (2019). *GAUSSIAN16*. Revision C.01. Gaussian Inc., Wallingford, CT, USA. https://gaussian.com/.
Glore, J. D., Hall, R. E. & Schram, E. P. (1972). *Inorg. Chem.* **11**, 550–553.
Groom, C. R., Bruno, I. J., Lightfoot, M. P. & Ward, S. C. (2016). *Acta Cryst.* B**72**, 171–179.
Hall, R. E. & Schram, E. P. (1969). *Inorg. Chem.* **8**, 270–274.
Hamilton, W. C. (1965). *Acta Cryst.* **18**, 502–510.
Jelsch, C., Guillot, B., Lagoutte, A. & Lecomte, C. (2005). *J. Appl. Cryst.* **38**, 38–54.
Koga, T., Kanayama, K., Watanabe, S. & Thakkar, A. J. (1999). *Int. J. Quant. Chem.* **71**, 491–497.
Loukhovitski, B. I., Sharipov, A. S. & Starik, A. M. (2016). *Eur. Phy. J. D*, **70**, 1–16.
Loukhovitski, B. I., Torokhov, S. A., Loukhovitskaya, E. E. & Sharipov, A. S. (2018). *Struct. Chem.* **29**, 49–68.
McArdle, P. (2019). *J. Chem. Educ.* **96**, 1412–1417.
Meenashi, R., Selvaraju, K., Stephen, A. D. & Jelsch, C. (2020). *J. Mol. Struct.* **1213**, 128139.
Parkin, G. (2019). *J. Chem. Educ.* **96**, 2467–2475.
Schram, E. P. & Hall, R. E. (1971). *Inorg. Chem.* **10**, 192–195.
Schram, E. P., Hall, R. E. & Glore, J. (1969). *J. Am. Chem. Soc.* **91**, 6643–6648.

Sheldrick, G. M. (2015). *Acta Cryst.* C**71**, 3–8.
Spackman, M. A. & Jayatilaka, D. (2009). *CrystEngComm*, **11**, 19–32.
Stewart, R. F. (1970). *J. Chem. Phys.* **53**, 205–213.
Tan, S. L., Jotani, M. M. & Tiekink, E. R. T. (2019). *Acta Cryst.* E**75**, 308–318.
Turner, M. J., Mckinnon, J. J., Wolff, S. K., Grimwood, D. J., Spackman, P. R., Jayatilaka, D. & Spackman, M. A. (2017). *Crystal Explorer17*. The University of Western Australia. https://crystalexplorer.net/.
Westrip, S. P. (2010). *J. Appl. Cryst.* **43**, 920–925.

supporting information

Acta Cryst. (2023). C**79**, 12-17 [https://doi.org/10.1107/S2053229622011391]

Structure and charge analysis of a cyclic aluminium hydride: *cyclo*-1,5-bis-μ-dimethylamino-3,7-di-μ-hydrido-2,4,6,8-tetrakis(dimethylaluminium)

Peter W. R. Corfield and Joshua Schrier

Computing details

Data collection: Corfield & Gainsford (1972); cell refinement: Corfield & Gainsford (1972); data reduction: Data reduction followed procedures in Corfield *et al.* (1973) with p = 0.06; program(s) used to solve structure: structure solved by heavy atom method with local programs; program(s) used to refine structure: *SHELXL2018* (Sheldrick, 2015); molecular graphics: *ORTEPIII* (Burnett & Johnson, 1996) and *ORTEP-3* (Farrugia, 2012); software used to prepare material for publication: *publCIF* (Westrip, 2010).

cyclo-Di-μ-dimethylamino-1:2κ^2N:*N*;3:4κ^2N:*N*-di-μ-hydrido-1:4κ^2H:*H*;2:3κ^2N:*N*-octamethyl-1κ^2C,2κ^2C,3κ^2C,4κ^2C-tetraaluminium

Crystal data

$[Al_4(CH_3)_8(C_2H_7N)_2H_2]$
M_r = 318.36
Monoclinic, $P2_1/n$
a = 14.175 (13) Å
b = 10.378 (11) Å
c = 7.692 (7) Å
β = 90.74 (4)°
V = 1131.5 (19) Å^3
Z = 2
$F(000)$ = 352
D_x = 0.934 Mg m^{-3}
Melting point: 371 K
Cu $K\alpha$ radiation, λ = 1.5418 Å
Cell parameters from 18 reflections
θ = 6.6–32.0°
μ = 1.83 mm^{-1}
T = 295 K
Block, white
0.48 × 0.40 × 0.17 mm

Data collection

Picker 4-circle diffractometer
Radiation source: sealed X-ray tube
Oriented graphite 200 reflection monochromator
$\theta/2\theta$ scans
Absorption correction: gaussian Busing & Levy (1957); 8 × 8 × 8 grid
T_{min} = 0.46, T_{max} = 0.71
3367 measured reflections
1582 independent reflections
1352 reflections with $I > 2\sigma(I)$
R_{int} = 0.068
θ_{max} = 58.0°, θ_{min} = 5.3°
h = −15→15
k = −11→11
l = 0→8
3 standard reflections every 120 reflections
intensity decay: 0(2)

Refinement

Refinement on F^2
Least-squares matrix: full
$R[F^2 > 2\sigma(F^2)]$ = 0.039
$wR(F^2)$ = 0.110
S = 1.07
1582 reflections
93 parameters
0 restraints

Primary atom site location: heavy-atom method
Secondary atom site location: difference Fourier map
Hydrogen site location: mixed
H atoms treated by a mixture of independent and constrained refinement
$w = 1/[\sigma^2(F_o^2) + (0.0374P)^2 + 0.310P]$ where $P = (F_o^2 + 2F_c^2)/3$

$(\Delta/\sigma)_{max} = 0.020$
$\Delta\rho_{max} = 0.18$ e Å^{-3}
$\Delta\rho_{min} = -0.20$ e Å^{-3}
Extinction correction: SHELXL2018 (Sheldrick, 2015), $Fc^* = kFc[1+0.001xFc^2\lambda^3/\sin(2\theta)]^{-1/4}$
Extinction coefficient: 0.0017 (6)

Special details

Geometry. All esds (except the esd in the dihedral angle between two l.s. planes) are estimated using the full covariance matrix. The cell esds are taken into account individually in the estimation of esds in distances, angles and torsion angles; correlations between esds in cell parameters are only used when they are defined by crystal symmetry. An approximate (isotropic) treatment of cell esds is used for estimating esds involving l.s. planes.

Fractional atomic coordinates and isotropic or equivalent isotropic displacement parameters (Å^2)

	x	*y*	*z*	U_{iso}*/U_{eq}
Al1	0.65285 (5)	0.51751 (7)	0.41280 (10)	0.0637 (3)
Al2	0.48132 (5)	0.72363 (7)	0.47924 (11)	0.0714 (3)
N1	0.61044 (13)	0.67245 (17)	0.5299 (2)	0.0604 (5)
C1	0.7692 (2)	0.4493 (3)	0.5148 (5)	0.1004 (10)
H1A	0.764793	0.449804	0.639229	0.151*
H1B	0.821432	0.501832	0.480213	0.151*
H1C	0.778652	0.362564	0.475149	0.151*
C2	0.6421 (2)	0.5293 (3)	0.1614 (4)	0.1014 (10)
H2A	0.578482	0.551219	0.129196	0.152*
H2B	0.658356	0.447829	0.110710	0.152*
H2C	0.684249	0.594546	0.120067	0.152*
C3	0.4321 (3)	0.8403 (3)	0.6563 (5)	0.1305 (14)
H3A	0.432406	0.797535	0.766972	0.196*
H3B	0.368677	0.864676	0.625666	0.196*
H3C	0.470986	0.915884	0.663073	0.196*
C4	0.4578 (3)	0.7665 (4)	0.2361 (5)	0.1150 (12)
H4A	0.446300	0.688924	0.171200	0.172*
H4B	0.511835	0.809927	0.190111	0.172*
H4C	0.403670	0.821806	0.226961	0.172*
C5	0.6745 (2)	0.7810 (3)	0.4799 (4)	0.0897 (9)
H5A	0.673112	0.791362	0.355897	0.134*
H5B	0.737792	0.761947	0.517927	0.134*
H5C	0.653740	0.859217	0.533990	0.134*
C6	0.6213 (2)	0.6521 (3)	0.7221 (3)	0.0858 (8)
H6A	0.582310	0.581384	0.757271	0.129*
H6B	0.602508	0.728784	0.782288	0.129*
H6C	0.686069	0.633178	0.749782	0.129*
H1	0.4342 (14)	0.5804 (18)	0.517 (2)	0.053 (5)*

Atomic displacement parameters (Å²)

	U^{11}	U^{22}	U^{33}	U^{12}	U^{13}	U^{23}
Al1	0.0583 (4)	0.0611 (5)	0.0718 (5)	−0.0003 (3)	−0.0012 (3)	0.0051 (3)
Al2	0.0704 (5)	0.0497 (4)	0.0941 (6)	0.0006 (3)	0.0036 (4)	0.0002 (4)
N1	0.0680 (12)	0.0534 (11)	0.0596 (11)	−0.0141 (9)	−0.0020 (9)	0.0055 (9)
C1	0.0787 (19)	0.104 (2)	0.118 (3)	0.0152 (17)	−0.0096 (18)	0.013 (2)
C2	0.107 (2)	0.118 (3)	0.0786 (19)	0.0213 (19)	0.0050 (17)	−0.0099 (18)
C3	0.138 (3)	0.086 (2)	0.168 (4)	0.020 (2)	0.034 (3)	−0.032 (2)
C4	0.112 (3)	0.114 (3)	0.118 (3)	0.022 (2)	−0.027 (2)	0.023 (2)
C5	0.0874 (19)	0.0711 (18)	0.110 (2)	−0.0281 (14)	−0.0003 (17)	0.0095 (16)
C6	0.104 (2)	0.090 (2)	0.0631 (16)	−0.0140 (16)	−0.0086 (15)	−0.0027 (14)

Geometric parameters (Å, º)

Al1—C2	1.941 (4)	C2—H2B	0.9600
Al1—N1	1.942 (3)	C2—H2C	0.9600
Al1—C1	1.950 (3)	C3—H3A	0.9600
Al1—H1^{i}	1.692 (19)	C3—H3B	0.9600
Al2—N1	1.941 (3)	C3—H3C	0.9600
Al2—C4	1.947 (4)	C4—H4A	0.9600
Al2—C3	1.958 (4)	C4—H4B	0.9600
Al2—H1	1.657 (19)	C4—H4C	0.9600
N1—C6	1.499 (3)	C5—H5A	0.9600
N1—C5	1.501 (3)	C5—H5B	0.9600
C1—H1A	0.9600	C5—H5C	0.9600
C1—H1B	0.9600	C6—H6A	0.9600
C1—H1C	0.9600	C6—H6B	0.9600
C2—H2A	0.9600	C6—H6C	0.9600
C2—Al1—N1	112.90 (12)	Al1—C2—H2C	109.5
C2—Al1—C1	118.58 (15)	H2A—C2—H2C	109.5
N1—Al1—C1	112.29 (13)	H2B—C2—H2C	109.5
C2—Al1—H1^{i}	107.9 (7)	Al2—C3—H3A	109.5
N1—Al1—H1^{i}	96.8 (7)	Al2—C3—H3B	109.5
C1—Al1—H1^{i}	105.7 (6)	H3A—C3—H3B	109.5
N1—Al2—C4	113.88 (13)	Al2—C3—H3C	109.5
N1—Al2—C3	111.93 (15)	H3A—C3—H3C	109.5
C4—Al2—C3	117.96 (18)	H3B—C3—H3C	109.5
N1—Al2—H1	95.8 (7)	Al2—C4—H4A	109.5
C4—Al2—H1	108.0 (7)	Al2—C4—H4B	109.5
C3—Al2—H1	106.5 (7)	H4A—C4—H4B	109.5
C6—N1—C5	107.7 (2)	Al2—C4—H4C	109.5
C6—N1—Al2	108.73 (17)	H4A—C4—H4C	109.5
C5—N1—Al2	108.40 (17)	H4B—C4—H4C	109.5
C6—N1—Al1	108.20 (17)	N1—C5—H5A	109.5
C5—N1—Al1	108.11 (18)	N1—C5—H5B	109.5
Al2—N1—Al1	115.49 (10)	H5A—C5—H5B	109.5

Al1—C1—H1A	109.5	N1—C5—H5C	109.5
Al1—C1—H1B	109.5	H5A—C5—H5C	109.5
H1A—C1—H1B	109.5	H5B—C5—H5C	109.5
Al1—C1—H1C	109.5	N1—C6—H6A	109.5
H1A—C1—H1C	109.5	N1—C6—H6B	109.5
H1B—C1—H1C	109.5	H6A—C6—H6B	109.5
Al1—C2—H2A	109.5	N1—C6—H6C	109.5
Al1—C2—H2B	109.5	H6A—C6—H6C	109.5
H2A—C2—H2B	109.5	H6B—C6—H6C	109.5
H1—Al2—N1—Al1	50.1 (7)	N1—Al2—C3—H3A	−61.1
Al1—N1—Al2—H1^{i}	30.4 (4)	N1—Al2—C4—H4A	82.9
N1—Al1—C1—H1A	44.9	Al1—N1—C5—H5A	58.4
N1—Al1—C2—H2A	−54.7	Al1—N1—C6—H6A	−61.8

Symmetry code: (i) −*x*+1, −*y*+1, −*z*+1.